Supporting Information

Gjorgjieva et al. 10.1073/pnas.1105933108

SI Text

Derivation of the Correlation Functions. We considered a feedforward network as in Fig. S1*A*. Let $x(t) = [x_1(t), \ldots, x_N(t)]^{\mathrm{T}}$ denote the vector of N inputs where $x_j(t) = \sum_{t_j^f} \delta(t - t_j^f)$ is the Dirac delta spike train of neuron j at time t, where t_j^f are the spike timings. The input spike trains have instantaneous firing rates $\rho^{\mathrm{inst}}(t) = [\rho_1^{\mathrm{inst}}(t), \ldots, \rho_N^{\mathrm{inst}}(t)]^{\mathrm{T}} = \langle x(t) \rangle$. (Here the expectation is taken over the input statistics.) The pairwise input correlation matrix (second moment) between inputs k and j is defined as

$$C_{kj}(s) = \frac{1}{T}\int_0^T \langle x_k(t) x_j(t-s) \rangle \mathrm{d}t. \qquad \text{[S1]}$$

[Formally, the correlation matrix should be written as $C_{kj}(t; s)$. For notational convenience, here we omit the dependence on t.] The diagonal elements of this pairwise input correlation matrix have an atomic (or point) discontinuity at $s = 0$ because $\langle x_k^2(t) \rangle = \langle x_k(t) \rangle \delta(0)$. [Note that in discrete time with bin size δt, we trivially have $x_k^2(t) = x_k(t)\delta t^{-1}$, where $x_k(t) \in \{0, \delta t^{-1}\}$ is the k^{th} spike train at time t.] Separating this correlation matrix from the pairwise correlation matrix without atomic discontinuities, C_{kj}° (where the "o" superscript denotes the absence of such discontinuity), gives

$$C_{kj}(s) = C_{kj}^{\circ}(s) + \delta_{kj}\delta(s)\ \rho_k \qquad \text{[S2]}$$

where δ_{kj} is the Kronecker delta function $\delta_{kj} = 0$ if $k \neq j$ and $\delta_{kj} = 1$ if $k = j$, and the mean firing rate averaged over the duration of the trial T is $\rho_k = (1/T)\int_0^T \rho_k^{\mathrm{inst}}(t)\mathrm{d}t$. The third-order correlation input statistic is given by

$$U_{kjn}(s_1, s_2) = \frac{1}{T}\int_0^T \langle x_k(t) x_j(t-s_1) x_n(t-s_2) \rangle \mathrm{d}t. \qquad \text{[S3]}$$

For this third-order tensor, U_j denotes a matrix whose (k, n) element is U_{kjn}. This third-order correlation function has atomic discontinuities at $s_1 = 0$, $s_2 = 0$, and $s_1 = s_2$, and we can write

$$\begin{aligned} U_{kjn}(s_1, s_2) = U_{kjn}^{\circ}(s_1, s_2) &+ \delta_{kj}\delta_{jn}\ \delta(s_1)\delta(s_2 - s_1)\ \rho_j \\ &+ \delta_{kj}\ \delta(s_1) C_{jn}(s_2 - s_1) + \delta_{kn}\ \delta(s_2) C_{kj}(s_1) \\ &+ \delta_{jn}\ \delta(s_2 - s_1) C_{kn}(s_2), \end{aligned} \qquad \text{[S4]}$$

where $U_{kjn}^{\circ}(s_1, s_2)$ is the third-order correlation without atomic discontinuities and is equal to $\rho_k\rho_j\rho_n$ if the inputs have independent Poisson statistics.

Let $u(t)$ denote the membrane potential of the postsynaptic neuron,

$$u(t) = \sum_{k=1}^{N} w_k \int_0^{\infty} \varepsilon(r) x_k(t - r)\mathrm{d}r, \qquad \text{[S5]}$$

where $\varepsilon(r)$ denotes the excitatory postsynaptic potential (EPSP) kernel taken to be a decaying exponential, $1/\tau_e e^{-r/\tau_e}\Theta(r)$, and $\Theta(r)$ is the Heaviside step function such that $\Theta(r) = 1$ when $r > 0$ and $\Theta(r) = 0$ otherwise. Postsynaptic spikes were generated stochastically from the membrane potential (1, 2), such that the probability density of firing a spike at time t was given by a nonlinear transfer function depending on the membrane potential, $\langle y(t) \rangle = g(u(t))$. (Here the expectation was taken over the postsynaptic spike train statistics.) For additional simplicity, this function was approximated by the first-order expansion about u_0 in the rest of the calculations

$$g(u(t)) \approx g(u_0) + g'(u_0)(u(t) - u_0), \qquad \text{[S6]}$$

where the expected membrane potential averaged over the trial duration T was

$$u_0 = \frac{1}{T}\int_0^T \langle u(t) \rangle \mathrm{d}t = \sum_{k=1}^{N} w_k \rho_k. \qquad \text{[S7]}$$

We also denoted the mean postsynaptic firing rate with $\nu = g(u_0)$. We derive the pre-post correlation K_j (between one presynaptic and the postsynaptic train),

$$\begin{aligned} K_j(s) &= \frac{1}{T}\int_0^T \langle y(t) x_j(t-s) \rangle \mathrm{d}t \\ &= \frac{1}{T}\int_0^T \langle g(u(t)) x_j(t-s) \rangle \mathrm{d}t \\ &= \frac{1}{T}\int_0^T \Big[g(u_0)\rho_j(t-s) + g'(u_0) \langle u(t) x_j(t-s) \rangle \\ &\quad - g'(u_0) u_0 \rho_j(t-s) \Big] \mathrm{d}t \\ &= g(u_0)\rho_j + g'(u_0) \left(\frac{1}{T}\int_0^T \langle u(t) x_j(t-s) \rangle \mathrm{d}t - u_0\rho_j \right) \\ &= (g(u_0) - g'(u_0)u_0)\rho_j + g'(u_0) \sum_k w_k C_{kj}^{\varepsilon}(s) \\ &= g'(u_0) \sum_k w_k C_{kj}^{\varepsilon}(s) + \alpha(u_0)\rho_j, \end{aligned} \qquad \text{[S8]}$$

where $\alpha(u) = g(u) - g'(u)u$ and $C_{kj}^{\varepsilon}(s) = \int_0^{\infty} \varepsilon(s') C_{kj}(s - s')\mathrm{d}s'$. Note that $\alpha(u)$ vanishes when $g(u)$ is strictly linear ($g(u) = u$) and is independent of the weights if $g(u)$ is an affine function (i.e., a linear function plus a translation). When the transfer function is linear $g(u) = u$, then $\alpha(u_0) = 0$ and $K_j(s) = \sum_k C_{kj}^{\varepsilon}(s) w_k$. We have expressed this term in Fig. S1 *B* and *D* (red curve). Fig. S1*B* shows the pre-post correlation for independent Poisson inputs (no correlations) which only has an exponential causal component ($\Delta t > 0$), corresponding to the EPSP. The presence of input correlations in Fig. S1*D* contributes both a larger exponential causal component and a nonzero acausal component ($\Delta t < 0$) - here we have assumed exponentially-decaying input correlations symmetric about 0.

For the post–prepost correlation tensor Q, we ignore the case when the two postsynaptic spikes overlap ($s_2 = 0$) because it is accounted for in the contribution from the pair rule. Then

$$\begin{aligned} Q_j(s_1, s_2) &= \frac{1}{T}\int_0^T \langle y(t - s_2) x_j(t - s_1) y(t) \rangle \mathrm{d}t \\ &= \frac{1}{T}\int_0^T \langle g(u(t - s_2)) x_j(t - s_1) g(u(t)) \rangle \mathrm{d}t \\ &= g^2(u_0)\rho_j - (g'(u_0))^2 u_0^2 \rho_j - 2g'(u_0)(g(u_0) - g'(u_0)u_0)\ u_0\rho_j \\ &\quad + g'(u_0)(g(u_0) - g'(u_0)u_0) \\ &\quad \frac{1}{T}\int_0^T \left[\langle x_j(t - s_1) u(t) \rangle + \langle u(t - s_2) x_j(t - s_1) \rangle \right] \mathrm{d}t \\ &\quad + (g'(u_0))^2 \frac{1}{T}\int_0^T \langle u(t) u(t - s_2) x_j(t - s_1) \rangle \mathrm{d}t. \end{aligned} \qquad \text{[S9]}$$

Using the expression for $\alpha(u)$ above, we get

$$Q_j(s_1,s_2) = \alpha(u_0)g'(u_0)\left(\frac{1}{T}\int_0^T \langle x_j(t-s_1)u(t)\rangle \mathrm{d}t + \frac{1}{T}\int_0^T \langle u(t-s_2)x_j(t-s_1)\rangle \mathrm{d}t\right) + (g'(u_0))^2\left(\frac{1}{T}\int_0^T \langle u(t)u(t-s_2)x_j(t-s_1)\rangle \mathrm{d}t\right) + \alpha^2(u_0)\rho_j. \quad \textbf{[S10]}$$

Now using Eq. **S7**, we get

$$Q_j(s_1,s_2) = \alpha(u_0)g'(u_0)\sum_k w_k\left(C^e_{kj}(s_1) + C^e_{kj}(s_1-s_2)\right) + (g'(u_0))^2\sum_{k,n} w_k w_n U^e_{kjn}(s_1,s_2) + \alpha^2(u_0)\rho_j, \quad \textbf{[S11]}$$

where $U^\varepsilon_j(s_1,s_2) = \int_0^\infty\int_0^\infty \varepsilon(r)\varepsilon(q)U_j(s_1-r,s_2-r+q)\mathrm{d}r\,\mathrm{d}q$. When the transfer function is linear $g(u) = u$, then $\alpha(u_0) = 0$; the pre-post-post correlation Q_j is simply a function of the (convolved) third-order input correlation tensor: $Q_j(s_1,s_2) = \sum_k\sum_n w_k w_n U^\varepsilon_{kjn}(s_1,s_2)$. This post-pre-post correlation is illustrated in Fig. S1*C* (*Right*) for independent Poisson inputs; due to the absence of correlations, the only nonzero component is for triplets in which the presynaptic spike occurs before the two postsynaptic spikes ($\Delta t_1 > \Delta t_2 > 0$). For correlated inputs with symmetric exponentially-decaying correlations, the component corresponding to pre-post-post triplet has a larger amplitude (Fig. S1*E*, *Right*), but here post-pre-post triplets ($\Delta t_2 > \Delta t_1 > 0$) also contribute to the correlation function.

Weight Dynamics. The triplet spike-timing–dependent plasticity (STDP) model can be written in the following differential form. Let $\bar{x}_j$ be a low-pass filtered version of the jth presynaptic spike train x_j with time constant τ_+ given by

$$\dot{\bar{x}}_j = -\frac{\bar{x}_j}{\tau_+} + x_j, \quad j = 1,\ldots,N. \quad \textbf{[S12]}$$

Similarly, let $\bar{y}_1$ and $\bar{y}_2$ be two different low-pass filtered versions of the postsynaptic spike train y with time constants τ_- and τ_y, respectively:

$$\dot{\bar{y}}_1 = -\frac{\bar{y}_1}{\tau_-} + y, \quad \textbf{[S13]}$$

$$\dot{\bar{y}}_2 = -\frac{\bar{y}_2}{\tau_y} + y. \quad \textbf{[S14]}$$

The minimal triplet STDP model can be written as

$$\dot{w}_j = -A_2^- x_j \bar{y}_1 + A_3^+ y \bar{x}_j \bar{y}_2. \quad \textbf{[S15]}$$

In the previous section we assumed that the weights w_j were fixed. Here, we allowed the weights to be dynamic, but with a small learning rate such that the results in the previous section are still valid (1, 2). Consistent with the approach of ref. 1, we expressed the weight change as a Volterra expansion of both the pre- and postsynaptic spike trains. Setting the first order terms to zero (because they correspond to non-Hebbian dynamics), we assumed that synaptic plasticity depends on second- and third-order terms only, i.e. pairs of spikes (1 pre and 1 post) and triplets of spikes (1 pre and 2 post)

$$\dot{w}_j = y(t)\int_0^\infty W_2(s)x_j(t-s)\mathrm{d}s + x_j(t)\int_0^\infty W_2(-s)y(t-s)\mathrm{d}s + y(t)\int_0^\infty\int_0^\infty W_3(s_1,s_2)x_j(t-s_1)y(t-s_2)\mathrm{d}s_1\mathrm{d}s_2$$

where W_2 is pair-based STDP and W_3 is triplet STDP (equations and parameters listed in the main text). [Note that in ref. 3, the wrong number of pairs is assumed in the STDP experiments (60 instead of 75) and therefore the fitted amplitude parameters were overestimated by approximately 10 %. For the sake of consistency with ref. 3 we kept the same parameters.] Assuming slow learning relative to the neuronal dynamics, and replacing the weights by their expectation averaged over a time period T, we have

$$\dot{w}_j = \int_{-\infty}^\infty W_2(s)K_j(s)\mathrm{d}s + \int_{-\infty}^\infty\int_{-\infty}^\infty W_3(s_1,s_2)Q_j(s_1,s_2)\mathrm{d}s_1\mathrm{d}s_2. \quad \textbf{[S16]}$$

Under the assumption of a linear approximation of the transfer function given in Eq. **S6**, and by inserting Eqs. **S8** and **S11** into Eq. **S16**, we find

$$\dot{w} = g'(u_0)(A+D)w + g'^2(u_0)\sum_{j=1}^N (w^{\mathrm{T}}B_j w)e_j + \kappa(u_0)\rho, \quad \textbf{[S17]}$$

where e_j is a vector of zeros with a 1 at the j^{th} component and

$$A_{jk} = \int_{-\infty}^\infty W_2(s)C^e_{kj}(s)\mathrm{d}s, \quad \textbf{[S18]}$$

$$D_{jk} = \alpha(u_0)\int_{-\infty}^\infty\int_{-\infty}^\infty W_3(s_1,s_2)\left(C^e_{kj}(s_1) + C^e_{kj}(s_1-s_2)\right)\mathrm{d}s_1\mathrm{d}s_2, \quad \textbf{[S19]}$$

$$B_{kjn} = \int_{-\infty}^\infty\int_{-\infty}^\infty W_3(s_1,s_2)U^e_{kjn}(s_1,s_2)\mathrm{d}s_1\mathrm{d}s_2, \quad \textbf{[S20]}$$

$$\kappa(u_0) = \alpha(u_0)\overline{W}_2 + \alpha^2(u_0)\overline{W}_3, \quad \textbf{[S21]}$$

with $\overline{W}_2 = \int_{-\infty}^\infty W_2(s)\mathrm{d}s$ and $\overline{W}_3 = \int_0^\infty\int_0^\infty W_3(s_1,s_2)\mathrm{d}s_1\mathrm{d}s_2$. Note that $g'(u_0)$ and $\kappa(u_0)$ depend on the weights w (through u_0), and therefore we cannot analyze Eq. **S17** in the same way as if we assume a strictly linear transfer function. In that case, with a linear transfer function, $g(u) = u$, we have $g'(u_0) = 1$, $\alpha(u_0) = 0$, and hence $\kappa(u_0) = 0$. Then we get:

$$\dot{w} = Aw + \sum_{j=1}^N (w^{\mathrm{T}}B_j w)e_j. \quad \textbf{[S22]}$$

We can also write this equation so that it resembles the Bienenstock–Cooper–Munro (BCM) equation for weight evolution (see also Eq. 6 in the main text),

$$\dot{w} = \underbrace{\phi(\nu)\rho}_{\text{BCM term}} + \Delta A w + \sum_{j=1}^N (w^{\mathrm{T}}\Delta B_j w)e_j, \quad \textbf{[S23]}$$

where $\phi(\nu) = \overline{W}_2\nu + \overline{W}_3\nu^2$ corresponds to the BCM term. The new covariance terms ΔA and ΔB are defined analogously to A and B given the input covariances,

$$\Delta A_{jk} = \int_{-\infty}^\infty W_2(s)\Delta C^e_{kj}(s)\mathrm{d}s, \quad \textbf{[S24]}$$

where $\Delta C_{kj}(s) = C_{kj}(s) - \rho_k\rho_j$ is the input pairwise covariance matrix, and

$$\Delta B_j = \int_0^\infty\int_0^\infty W_3(s_1,s_2)\Delta U^e_j(s_1,s_2)\mathrm{d}s_1\mathrm{d}s_2,$$

where $\Delta U_{kjn}(s_1, s_2) = U_{kjn}(s_1, s_2) - \rho_k\rho_j\rho_n$ is the input triplet covariance tensor.

M patterns were presented to the network, pattern i with probability p_i, with a mean firing rate of $\rho^{(i)}$ and pairwise and triplet correlations terms $A^{(i)}$ and $B^{(i)}$, respectively. To match the triplet rule to the BCM model, we set $A_2^- \to A_2^-\,\overline{\nu}/\rho_0^p$, where the expectation of the p^{th} power of the postsynaptic firing rate can be expressed as $\overline{\nu} = \sum_{i=1}^{M} p_i(\nu^{(i)})^p$. This quantity was approximated by low-pass filtering the p^{th} power of the instantaneous postsynaptic firing rate $\nu(t) = g(u(t))$ with a time constant which has to be larger than M times the frequency of pattern presentation, i.e. $r \simeq \overline{\nu}$ where $\tau_r\dot{r} = -r + \nu^p$ with a time constant of $\tau_r = 5$s. For all the calculations in this paper we took $p = 2$. Using the minimal triplet model of ref. 3 where $A_2^+ = 0$, $A^{(i)}$ contains only depression effects from the pair STDP rule ($A_2^- \neq 0$) such that the weight equation becomes

$$\dot{w} = \sum_{i=1}^{M} p_i \left(\phi\left(\nu^{(i)}, \overline{\nu}\right)\rho^{(i)} + \Delta A^{(i)}(\overline{\nu})w + \sum_{j=1}^{N}\left(w^{\mathrm{T}}\Delta B_j^{(i)}w\right)e_j \right). \quad \text{[S25]}$$

Here, $\nu^{(i)} = w^{\mathrm{T}}\rho^{(i)}$ denotes the average postsynaptic firing rate elicited by pattern i.

Selectivity with N Orthogonal Rate-Based Input Patterns. In the case of M=N orthogonal Poisson inputs we show that the maximally selective fixed points of the weight dynamics driven by the triplet learning rule are stable. Because we consider patterns with positive components (rates), the Poisson rate of the j^{th} component of pattern i is given by $\rho_j^{(i)} = \delta_{ij}|\rho^{(i)}|$ (i.e., pattern i has all zero components but the i^{th} component).

Because of the Poisson assumption, we have $\Delta C_{kj}(s) = \delta_{kj}\delta(s)\rho_k$ and hence $\Delta C_{kj}^{\varepsilon}(s) = \delta_{kj}\,\rho_k\varepsilon(s) = 0$ for $s < 0$. Because we use the minimal triplet model (for which $A_2^+ = 0$), $W_2(s) = 0$ for $s \geq 0$. As a consequence, ΔA vanishes because it is obtained by integrating the product $W_2(s)\cdot\Delta C_{kj}^{\varepsilon}(s)$ (Eq. **S24**). By using Eqs. **S4** and **S11**, $\Delta B_{kjn}^{(i)}$ can be written as

$$\Delta B_{kjn}^{(i)} = \left(b_1\delta_{kj}\rho_n^{(i)} + b_2\delta_{kn}\rho_k^{(i)} + b_3\delta_{kj}\delta_{kn}\right)\rho_j^{(i)}, \quad \text{[S26]}$$

where

$$b_1 = \int_0^\infty\int_0^\infty W_3(s_1, s_2)(\varepsilon(s_1) + \varepsilon(s_2 - s_1))\mathrm{d}s_1\,\mathrm{d}s_2, \quad \text{[S27]}$$

$$b_2 = \int_0^\infty\int_0^\infty W_3(s_1, s_2)\int_0^\infty \varepsilon(r)\varepsilon(r - s_2)\mathrm{d}r\,\mathrm{d}s_1\,\mathrm{d}s_2, \quad \text{[S28]}$$

and

$$b_3 = \int_0^\infty\int_0^\infty W_3(s_1, s_2)\varepsilon(s_1)\varepsilon(s_2 - s_1)\mathrm{d}s_1\mathrm{d}s_2. \quad \text{[S29]}$$

In the presence of $M = N$ Poisson patterns, we can write the expected weight dynamics as

$$\dot{w} = \sum_{i=1}^{M} p_i\left(\phi\left(\nu^{(i)}, \overline{\nu}\right)\mathbf{1} + \Lambda^{(i)}\right)\rho^{(i)}, \quad \text{[S30]}$$

where

$$\phi\left(\nu^{(i)}, \overline{\nu}\right) = \overline{W}_2\frac{\overline{\nu}}{\rho_0^2}\nu^{(i)} + \overline{W}_3\left(\nu^{(i)}\right)^2, \quad \text{[S31]}$$

$\mathbf{1}$ is the $N \times N$ identity matrix, and $\Lambda^{(i)}$ is a diagonal matrix where the j^{th} diagonal element is

$$\Lambda_{jj}^{(i)} = \left(b_1 w_j\nu^{(i)} + b_2\nu_2^{(i)} + b_3 w_j^2\right)\rho_j^{(i)} \quad \text{[S32]}$$

with $\nu_2^{(i)} = \sum_k w_k^2\rho_k^{(i)}$. Recall that $\overline{\nu} = \sum_i p_i(\nu^{(i)})^2$ with $\nu^{(i)} = w^{\mathrm{T}}\rho(i)$. Because of the orthogonality assumption, the condition $\dot{w} = 0$ implies that $\phi(\nu^{(i)}, \overline{\nu}^{(i)}) + \Lambda_{ii}^{(i)} = 0$, for all $i = 1, \ldots, N$ and therefore

$$w_i^2 F\left(\rho_i^{(i)}\right) - G\rho_i^{(i)}w_i\overline{\nu} = 0, \quad \forall i = 1, \ldots, N, \quad \text{[S33]}$$

where

$$G = -\frac{\overline{W}_2}{\rho_0^2} > 0 \text{ and } F\left(\rho_i^{(i)}\right) = \overline{W}_3\left(\rho_i^{(i)}\right)^2 + (b_1 + b_2)\rho_i^{(i)} + b_3. \quad \text{[S34]}$$

Each fixed point of Eq. **S30** must satisfy the N conditions from Eq. **S33**. Each condition has two solutions: either $w_i^* = 0$ or $w_i^* = G\rho_i^{(i)}/F(\rho_i^{(i)})$. As a consequence, there are 2^N fixed points, which is consistent with the BCM theory.

It remains to be shown that the maximally selective fixed points are stable. The n^{th} fixed point is given by

$$w^{\star(n)} = (0, \ldots, 0,\ w_n^*,\ 0, \ldots, 0)^{\mathrm{T}},$$

where

$$w_n^* = \frac{F\left(\rho_n^{(n)}\right)}{Gp_n\left(\rho_n^{(n)}\right)^3} \text{ takes the } n^{\text{th}} \text{ position.}$$

To demonstrate that this fixed point is stable, we have to show that the eigenvalues of the Jacobian of Eq. **S30** are negative when evaluated at $w^{*(n)}$. We find that this Jacobian matrix is given by

$$J_{ij}\left(w^{\star(n)}\right) = -\delta_{ij}p_i G\left(\rho_i^{(i)}\right)^2\overline{\nu}^{(n)}, \quad \text{[S35]}$$

where $\overline{\nu}^{(n)} = p_n w_n^2(\rho_n^{(n)})^2$. Because this matrix is diagonal with all diagonal elements being negative, we conclude that all of the maximally selective fixed points are stable.

At this fixed point, the sliding threshold takes the value

$$\theta = w^{\star(n)}\rho_n^{(n)} = \theta_0(\overline{\nu})\left(1 + \left(\tau_1\rho_n^{(n)}\right)^{-1} + \left(\tau_2\rho_n^{(n)}\right)^{-2}\right)^{-1}, \quad \text{[S36]}$$

where $\theta_0(\overline{\nu}) = A_2^-\,\tau_-\,\overline{\nu}/(A_3^+\tau_+\tau_y\rho_0^p)$ is the sliding threshold of the BCM term only when the correlation terms can be neglected (i.e., $\Delta A = 0$ and $\Delta B = 0$). The new timescales are

$$\tau_1 = \overline{W}_3/(b_1 + b_2) \text{ and } \tau_2 = \sqrt{\overline{W}_3/b_3}. \quad \text{[S37]}$$

One can calculate these values and obtain

$$\frac{b_1 + b_2}{\overline{W}_3} = \frac{1}{\tau_m + \tau_+} + \frac{\tau_+}{(\tau_m + \tau_+)(\tau_+ + \tau_y)} + \frac{1}{2(\tau_m + \tau_y)} \quad \text{[S38]}$$

and

$$\frac{b_3}{\overline{W}_3}=\frac{\tau_+}{(\tau_m+2\tau_+)(\tau_+\tau_y+\tau_m\tau_++\tau_m\tau_y)}, \quad \text{[S39]}$$

where $\overline{W}_3=A_3^+\tau_+\tau_y$. Note that in the limit where $\tau_m \simeq \tau_+ \simeq \tau_-$ and $\tau_y \gg \tau_m$, we have $\tau_1 \approx 2\tau_m$ and $\tau_2 \approx \sqrt{6\tau_m\tau_y}$.

Selectivity in a 2D System with Correlation-Based Input Patterns. We consider a 2D system where two patterns are presented to the feedforward network, each consisting of two pools of inputs: let $j = 1, \ldots, N/2$ denote the inputs from the first pool and $j = N/2 + 1, \ldots, N$ denote the inputs from the second pool. Let $\tilde{w}_j$ denote the weights in the network and $\tilde{A}^{(i)}$ and $\tilde{B}_k^{(i)}$ the convolved pairwise and third-order correlations of the inputs in each pool for pattern i, respectively, with the pair-based and the triplet STDP rules (Eqs. **S18** and **S20**). We further imposed a lower bound on the weights, $w \geq w_{\min} = 0$, which in the case of orthogonal rate-based patterns was automatically satisfied.

Under the assumption that the weights in each pool evolve together,

$$\tilde{w}_j \simeq w_1, j = 1, \ldots, \frac{N}{2}, \quad \text{[S40]}$$

$$\tilde{w}_j \simeq w_2, j = \frac{N}{2}+1, \ldots, N. \quad \text{[S41]}$$

Summing the weights in each pool of inputs for pattern $i = 1, 2$ gives

$$\sum_{j=1}^{N/2}\dot{\tilde{w}}_j=\frac{N}{2}\dot{w}_1=\sum_{j=1}^{N/2}\left(\sum_{k=1}^{N}\tilde{A}_{jk}^{(i)}\tilde{w}_k\frac{\overline{\nu}}{\rho_0^2}+\sum_{m=1}^{N}\sum_{n=1}^{N}\tilde{w}_m\tilde{w}_n\left(\tilde{B}_j^{(i)}\right)_{mn}\right) \quad \text{[S42]}$$

$$\sum_{j=N/2+1}^{N}\dot{\tilde{w}}_j=\frac{N}{2}\dot{w}_2=\sum_{j=\frac{N}{2}+1}^{N}\left(\sum_{k=1}^{N}\tilde{A}_{jk}^{(i)}\tilde{w}_k\frac{\overline{\nu}}{\rho_0^2}+\sum_{m=1}^{N}\sum_{n=1}^{N}\tilde{w}_m\tilde{w}_n\left(\tilde{B}_j^{(i)}\right)_{mn}\right). \quad \text{[S43]}$$

The contributions from the pairwise correlations are given by

$$A_{11}^{(i)}=\frac{2}{N}\sum_{j=1}^{N/2}\sum_{k=1}^{N/2}\tilde{A}_{jk}^{(i)},\ A_{12}^{(i)}=\frac{2}{N}\sum_{j=1}^{N/2}\sum_{k=\frac{N}{2}+1}^{N}\tilde{A}_{jk}^{(i)},$$

$$A_{21}^{(i)}=\frac{2}{N}\sum_{j=\frac{N}{2}+1}^{N}\sum_{k=1}^{N/2}\tilde{A}_{jk}^{(i)},\ A_{22}^{(i)}=\frac{2}{N}\sum_{j=N/2+1}^{N}\sum_{k=\frac{N}{2}+1}^{N}\tilde{A}_{jk}^{(i)}$$

for pattern $i = 1, 2$, where the average postsynaptic rate over all of the patterns is

$$\overline{\nu}=p_1\left(\rho_1^{(1)}w_1+\rho_2^{(1)}w_2\right)^2+p_2\left(\rho_1^{(2)}w_1+\rho_2^{(2)}w_2\right)^2 \quad \text{[S44]}$$

with

$$\rho_1^{(i)}=\left(\sum_{j=1}^{N/2}\tilde{\rho}_j^{(i)}\right),\ \rho_2^{(i)}=\left(\sum_{j=N/2+1}^{N}\tilde{\rho}_j^{(i)}\right).$$

The terms involving the third-order correlations are

$$\left(B_1^{(i)}\right)_{11}=\frac{2}{N}\sum_{j=1}^{N/2}\sum_{m=1}^{N/2}\sum_{n=1}^{N/2}\left(\tilde{B}_j\right)_{mn},$$

$$\left(B_1^{(i)}\right)_{12}=\frac{2}{N}\sum_{j=1}^{N/2}\sum_{m=1}^{N/2}\sum_{n=N/2+1}^{N}\left(\tilde{B}_j\right)_{mn},$$

$$\left(B_1^{(i)}\right)_{21}=\frac{2}{N}\sum_{j=1}^{N/2}\sum_{m=\frac{N}{2}+1}^{N}\sum_{n=1}^{N/2}\left(\tilde{B}_j\right)_{mn},$$

$$\left(B_1^{(i)}\right)_{22}=\frac{2}{N}\sum_{j=1}^{N/2}\sum_{m=\frac{N}{2}+1}^{N}\sum_{n=\frac{N}{2}+1}^{N}\left(\tilde{B}_j\right)_{mn},$$

$$\left(B_2^{(i)}\right)_{11}=\frac{2}{N}\sum_{j=\frac{N}{2}+1}^{N}\sum_{m=1}^{N/2}\sum_{n=1}^{N/2}\left(\tilde{B}_j\right)_{mn},$$

$$\left(B_2^{(i)}\right)_{12}=\frac{2}{N}\sum_{j=\frac{N}{2}+1}^{N}\sum_{m=1}^{N/2}\sum_{n=\frac{N}{2}+1}^{N}\left(\tilde{B}_j\right)_{mn},$$

$$\left(B_2^{(i)}\right)_{21}=\frac{2}{N}\sum_{j=\frac{N}{2}+1}^{N}\sum_{m=\frac{N}{2}+1}^{N}\sum_{n=1}^{N/2}\left(\tilde{B}_j\right)_{mn},$$

$$\left(B_2^{(i)}\right)_{22}=\frac{2}{N}\sum_{j=\frac{N}{2}+1}^{N}\sum_{m=\frac{N}{2}+1}^{N}\sum_{n=\frac{N}{2}+1}^{N}\left(\tilde{B}_j\right)_{mn},$$

finally giving an equation for the weight dynamics of the two pools of inputs, corresponding to $M = 2$ in Eq. **S25**

$$\dot{w}=\sum_{i=1}^{2}p_i\left(A^{(i)}(\overline{\nu})w+\sum_{k=1}^{2}w^{\mathrm{T}}B_k^{(i)}we_k\right). \quad \text{[S45]}$$

Next, we derive the fixed points of the 2D system of Eq. **S45** using $\overline{\nu}=\sum_{i=1}^{2}p_i(w^{\mathrm{T}}\rho^{(i)})^2$. To obtain the general fixed points of this equation, we have to simultaneously solve $\dot{w}_1 = 0$ and $\dot{w}_2 = 0$. This process amounts to solving two cubic equations for which we do not get nice analytical expressions. Fortunately, the fixed points of interest [the ones associated with maximal selectivity, i.e., $(w_1^*, 0)$ and $(0, w_2^*)$ with $w_1^*, w_2^* > 0$] are simpler to express. To find a fixed point on the w_1 axis, we solve $\dot{w}_1 = 0$ at $w_1 = w_1^*$ and $w_2 = 0$,

$$0=p_1\left[A_{11}^{(1)}w_1\frac{p_1\left(w^{\mathrm{T}}\rho^{(1)}\right)^2+p_2\left(w^{\mathrm{T}}\rho^{(2)}\right)^2}{\rho_0^2}+\left(B_1^{(1)}\right)_{11}w_1^2\right]+p_2\left[A_{11}^{(2)}w_1\frac{p_1\left(w^{\mathrm{T}}\rho^{(1)}\right)^2+p_2\left(w^{\mathrm{T}}\rho^{(2)}\right)^2}{\rho_0^2}+\left(B_1^{(2)}\right)_{11}w_1^2\right], \quad \text{[S46]}$$

which gives the linear equation

$$\left(p_1A_{11}^{(1)}+p_2A_{11}^{(2)}\right)\frac{p_1\left(\rho_1^{(1)}\right)^2+p_2\left(\rho_1^{(2)}\right)^2}{\rho_0^2}w_1^*+\left(p_1\left(B_1^{(1)}\right)_{11}+p_2\left(B_1^{(2)}\right)_{11}\right)=0. \quad \text{[S47]}$$

This equation has the solution

$$w_1^*=-\frac{p_1\left(B_1^{(1)}\right)_{11}+p_2\left(B_1^{(2)}\right)_{11}}{\rho_0^{-2}\left(p_1A_{11}^{(1)}+p_2A_{11}^{(2)}\right)p_1\left(\rho_1^{(1)}\right)^2+p_2\left(\rho_1^{(2)}\right)^2}. \quad \text{[S48]}$$

The expression for w_2^* can be similarly obtained. Instead of examining the Jacobian of the system at the fixed points to obtain their stability, because of the nonlinearity due to the lower

bound on the weights, we require that the following two conditions be satisfied for stability (where the system is denoted by $\dot{w} = F(w)$):

$$\left.\frac{\partial F_1(w)}{\partial w_1}\right|_{w=w^*} < 0, \qquad \text{[S49]}$$

$$F_2(w^*) < 0. \qquad \text{[S50]}$$

The first condition becomes

$$3\left(p_1 A_{11}^{(1)} + p_2 A_{11}^{(2)}\right)\frac{p_1\left(\rho_1^{(1)}\right)^2 + p_2\left(\rho_1^{(2)}\right)^2}{\rho_0^2} w_1^* + 2\left(p_1\left(B_1^{(1)}\right)_{11} + p_2\left(B_1^{(2)}\right)_{11}\right) < 0. \qquad \text{[S51]}$$

If we use the expression for w_1^* from Eq. **S48**, then the condition reduces to

$$p_1\left(B_1^{(1)}\right)_{11} + p_2\left(B_1^{(2)}\right)_{11} > 0, \qquad \text{[S52]}$$

which is always true because the correlation terms convolved with the triplet rule in $B_k^{(i)}$ are always positive.

The second condition becomes

$$\left(p_1 A_{21}^{(1)} + p_2 A_{21}^{(2)}\right)\frac{p_1\left(\rho_1^{(1)}\right)^2 + p_2\left(\rho_1^{(2)}\right)^2}{\rho_0^2} w_1^* + \left(p_1\left(B_2^{(1)}\right)_{11} + p_2\left(B_2^{(2)}\right)_{11}\right) < 0. \qquad \text{[S53]}$$

If we use the expression for w_1^* from Eq. **S48**, the condition reduces to

$$\frac{p_1 A_{21}^{(1)} + p_2 A_{21}^{(2)}}{p_1 A_{11}^{(1)} + p_2 A_{11}^{(2)}} > \frac{p_1\left(B_2^{(1)}\right)_{11} + p_2\left(B_2^{(2)}\right)_{11}}{p_1\left(B_1^{(1)}\right)_{11} + p_2\left(B_1^{(2)}\right)_{11}}. \qquad \text{[S54]}$$

Similarly, the fixed point on the w_2 axis is stable if the following condition holds:

$$\frac{p_1 A_{12}^{(1)} + p_2 A_{12}^{(2)}}{p_1 A_{22}^{(1)} + p_2 A_{22}^{(2)}} > \frac{p_1\left(B_1^{(1)}\right)_{22} + p_2\left(B_1^{(2)}\right)_{22}}{p_1\left(B_2^{(1)}\right)_{11} + p_2\left(B_2^{(2)}\right)_{22}}. \qquad \text{[S55]}$$

Numerical evaluations of these two conditions for a large variety of firing rates and pairwise and third-order correlations have demonstrated that the conditions always hold. Therefore, in the case of a 2D network, the system always results in selectivity. As we show in the main text, this is not always the case for a general N-dimensional system, where selectivity depends on the input correlation structure.

Numerical Simulations with Multiple Patterns. For the simulations with rate-based patterns in Fig. 2, the inputs within each pattern were given independent Poisson spike trains lacking correlations. For each of 10 patterns uniformly spaced and centered at inputs 5, 15, … 95, a Gaussian rate profile was used with a background firing rate of $r_{\min}$ and a peak firing rate of $r_{\max}$, and we explored three ratios in Fig. 2*B*: $r_{\min}/r_{\max} = \{0/55, 5/55, 10/55\}$. The SD of the Gaussian was also varied in Fig. 2, $\sigma = \{5.0, 7.5, 10.0, 12.5, 15.0\}$, but the Gaussian profile was normalized such that it generated the same postsynaptic firing rate for each value of σ and $r_{\min}/r_{\max}$. The postsynaptic neuron was linear $g(u) = 10u$ and the target postsynaptic firing rate was set to $\rho_0 = 8.5$ Hz.

For the simulations with correlation-based patterns in Fig. 3, each of the 100 inputs had the same firing rate of 10 Hz. In each pattern, 90 inputs were given independent Poisson spikes, and 10 inputs had uniform correlations between any pair and triplet of inputs. For the spatial correlations in Fig. 3*B*, each pair and triplet of inputs shared 90% identical spikes. For the spatiotemporal correlations in Fig. 3*C*, half of the 90% shared spikes for each pair and triplet of inputs were shifted by an exponential random distribution with a mean of 5 ms resulting in symmetric, exponentially-decaying correlations with a timescale of 5 ms. For simplicity, we assumed uniform correlations for all input pairs and triplets. The postsynaptic neuron was linear $g(u) = 10\ u$ and the target postsynaptic firing rate was set to $\rho_0 = 10.5$ Hz.

For the simulations in Fig. 4 *A–C*, there were two patterns consisting of three inputs each, with the same firing rates and pairwise correlations, but with different third-order correlations. The postsynaptic neuron was linear $g(u) = 50\ u$ and the target postsynaptic firing rate was 20 Hz. For Fig. 4*D*, a network of two groups of five neurons each was simulated so that the two input groups had the same lower-order correlations (for example, same firing rates, pairwise and third-order correlations), but differed in the presence or absence of higher-order correlations in each group (corresponding example, fourth- and fifth-order correlations). The correlated spike trains in Fig. 3 and 4 were generated using the mixture method described in ref. 4 (see next section).

In Figs. 2–5, a new randomly-chosen pattern was presented to the network every 200 ms. Pre- and postsynaptic spikes were simulated stochastically given the respective firing rates. The initial weights were set to 1 and hard bounds were set between 0 and 3 (in Fig. 4 because of the small number of inputs the bounds were five times larger.) Postsynaptic activity was low-pass filtered with a time constant of 5 seconds. A_2^+ and A_3^- were reduced by a factor of 10 compared to the parameters in ref. 3 to give smooth evolution of the weights, but this did not affect the results.

Simulations of Correlated Spike Trains. Correlated spike trains in Figs. 3 and 4 in the main text were simulated by using the mixture method following Brette (3). The general method is illustrated in Fig. S2, where N target spike trains (gray) are generated from M source trains (blue), with specifics adjusted to fit our simulations. Fig. S2*A* illustrates the method for generating correlated spike trains with pairwise correlations only, and Fig. S2*B* shows the method for generating correlated spike trains with pairwise and third-order correlations. Both methods were used in Fig. 4 *B* and *C* for simulating 6 spike trains with $N = 3$ for each method (in Fig. 4*D* we used 10 spike trains with $N = 5$) and $M = N$ in Fig. S2*A* and $M = N + 1$ in Fig. S2*B*, whereas the method in Fig. S2*B* was used in Fig. 3 with $M = N = 100$. The source trains were independent Poisson processes with rate R. Spikes from source train m were copied into target train m with probability p_1. Furthermore, to generate instantaneous correlations among the target spike trains, spikes from the common source spike trains were copied into the the target trains. In Fig. S2*B*, spikes were copied from the single common spike train, generating correlations of higher order in the target trains. In Fig. S2*A*, each pair of target trains received spikes from a single common course train (probability of copying p_2), different for each pair of target trains, thus generating only pairwise correlations among the target trains, but no higher-order correlations.

In both cases, the firing rate of the k^{th} target train is given by (3)

$$\rho_k = (p_1 + p_2)\, R. \qquad \textbf{[S56]}$$

The pairwise covariance matrix without the atomic discontinuities ΔC° can be defined analogously to the corresponding correlation matrix in Eq. **S2**:

$$\Delta C_{kj}(s) = \Delta C^\circ_{kj}(s) + \delta_{kj}\delta(s)\,\rho_j. \qquad \textbf{[S57]}$$

Then the instantaneous pairwise covariance is (see ref. 3 for details)

$$\Delta C^\circ_{kj}(s) = \gamma_{kj}\delta(s). \qquad \textbf{[S58]}$$

This covariance had the same magnitude for any pair of inputs k, j: For Fig. S2*A*, $\gamma_{kj} = p_1 p_2 R$ and for Fig. S2*B*, $\gamma_{kj} = p_2^2 R$.

The expression for the third-order covariance is more complicated [it can be related to U_{kjn} by $\Delta V_{kjn}(s_1, s_2) = U_{kjn}(s_1, s_2) - \rho_k \Delta C_{jn}(s_2 - s_1) - \rho_j \Delta C_{kn}(s_2) - \rho_n \Delta C_{kj}(s_1) - \rho_k \rho_j \rho_n$]:

$$\Delta V_{kjn}(s_1, s_2) = \frac{1}{T}\int_0^T \Big\langle (x_k(t) - \rho_k)\Big(x_j(t - s_1) - \rho_j\Big)(x_n(t - s_2) - \rho_n)\Big\rangle \mathrm{d}t. \qquad \textbf{[S59]}$$

After separating the atomic discontinuities

$$\begin{aligned}\Delta V_{kjn}(s_1, s_2) =& \Delta V^\circ_{kjn}(s_1, s_2) + \delta_{kj}\delta_{jn}\delta(s_1)\delta(s_2 - s_1)\rho_j \\ &+ \delta_{kj}\delta(s_1)\Delta C^\circ_{jn}(s_2 - s_1) + \delta_{kn}\delta(s_2)\Delta C^\circ_{kj}(s_1) \\ &+ \delta_{jn}\delta(s_2 - s_1)\Delta C^\circ_{kn}(s_2),\end{aligned} \qquad \textbf{[S60]}$$

we can specify the instantaneous third-order covariance by (see ref. 3 for details)

$$\Delta V^\circ_{kjn}(s) = \lambda_{kjn}\delta(s_1)\delta(s_2). \qquad \textbf{[S61]}$$

This covariance had the same magnitude for any triplet of inputs k, j, n: For Fig. S2*A*, $\lambda_{kjn} = 0$ and for Fig. S2*B*, $\lambda_{kjn} = p_2^3 R$.

In Fig. 3, we used the method in Fig. S2*B* with $N = 100$, $R = 9.09$ Hz, and $p_1 = 0.1$ and $p_2 = 1.0$. In Fig. 4 *B* and *C*, we used both methods in Fig. S2 with $N = 3$, $R = 5$ Hz, and $p_1 = p_2 = 1.0$.

To show that in Fig. 4*C* of the main text these methods do indeed generate the same pairwise correlations (but different third-order correlations), we computed the mean ± SEM of the peak correlation coefficients for 200 simulation runs in each case (Fig. S3).

In Fig. 4*D*, we extended the methods described in Fig. S2 to generate correlations of higher than third order and considered $N = 5$ neurons per group. To illustrate the procedure, we describe how we generated correlated spikes to distinguish between correlations of fifth order. First we generated a single common source train (with rate R) from which spikes were copied into the target trains of the inputs in group 1 with probability p. This process generated the following statistics for the inputs in group 1: rates pR, pairwise correlations p^2R, third-order correlations p^3R, fourth-order correlations p^4R, and fifth-order correlations p^5R. Then we generated $\binom{5}{4} = 5$ source trains (with rates R), each copying spikes with probability p into the 4-tuplets of target trains (1, 2, 3, 4), (1, 2, 3, 5), (2, 3, 4, 5), (1, 2, 4, 5), (1, 3, 4, 5) in group 2. This process generated fourth-order correlations p^4R in group 2 (but no fifth-order correlations because no target trains received spikes from the same source train). Thus, the fifth-order correlations were different for groups 1 (p^5R) and 2 (0), but the fourth-order correlations were the same (p^4R). However, the lower-order correlations also differed. The third-order correlations in group 1 (p^3R) were lower than the third-order correlations in group 2 ($2p^3R$). Therefore, we generated $\binom{5}{3} = 10$ more source trains for the inputs in group 1, which copied spikes into the triplets of target trains (1, 2, 3), (1, 2, 4), (1, 2, 5), (1, 3, 4), (1, 3, 5), (1, 4, 5), (2, 3, 4), (2, 3, 5), (2, 4, 5), (3, 4, 5) in group 1. Now even the third-order correlations in both groups were matched to $2p^3R$. However, the pairwise correlations in group 1 then became $4p^2R$, whereas in group 2 they were $3p^2R$. To match these pairwise correlations, we generated $\binom{5}{2} = 10$ source trains in group 2, copying spikes into the pairs of target trains (1, 2), (1, 3), (1, 4), (1, 5) (2, 3), (2, 4), (2, 5), (3, 4), (3, 5), (4, 5) in group 2. Now the pairwise correlations in both groups 1 and 2 were matched to $4p^2R$. However, the firing rates for the target trains in group 1 were $7pR$, whereas for the target trains in group 2 they were $8pR$. Finally, we generated $\binom{5}{1} = 5$ more source trains in group 1 that copied spikes independently into each of the 5 target trains, giving firing rates in each group equal to $8pR$. Because the target firing rate was 10 Hz, all source trains had rates $10/(8p)$ Hz. For simplicity, we used a copying probability of $p = 1.0$, meaning that all of the spikes from the source trains were copied into the target trains. In this example, there were a total of 16 source trains generated for the 5 target trains in group 1 and 15 source trains for the 5 target trains in group 2. Analogous procedures were used for the cases with correlations of $k = 2$, 3, or 4$^{\text{th}}$ order. For the case of $k = 1$ we studied the difference in first-order correlations, i.e., firing rates, and thus we considered rates of 10 Hz in group 1 and 7 Hz in group 2.

For generating spatiotemporal correlations, the mixture method described by Brette (3) was used. The instantaneous correlated spike trains (generated as above) were shifted by independent and identically distributed random numbers from an appropriate distribution function. We used an exponential distribution with a time constant τ_c, $f(t) = (1/\tau_c)e^{-t/\tau_c}\Theta(t)$, where $\Theta(x)$ is the Heaviside function, such that

$$\Delta C^\circ_{kj}(s) = \gamma_{kj}\int_{-\infty}^{\infty} f(t)f(t - s)\mathrm{d}t = \frac{\gamma_{kj}}{2\tau_c}e^{-|s|/\tau_c} \qquad \textbf{[S62]}$$

and the third-order covariance

$$\begin{aligned}\Delta V^\circ_{kjn}(s_1, s_2) &= \lambda_{kjn}\int_{-\infty}^{\infty} f(t)f(t - s_1)f(t - s_2)\mathrm{d}t \\ &= \frac{\lambda_{kjn}}{3\tau_c^2}\begin{cases} e^{-(s_1+s_2)/\tau_c}, & s_1 \geq 0,\ s_2 \geq 0 \\ e^{(2s_1 - s_2)/\tau_c}, & s_1 < 0,\ s_2 > s_1 \\ e^{(-s_1+2s_2)/\tau_c}, & s_1 > s_2, s_2 < 0. \end{cases}\end{aligned} \qquad \textbf{[S63]}$$

Note that in all of the simulations in the main text we assumed uniform correlations for all spike pairs and triplets such that $\gamma_{kj} = \gamma$ for all pairs (k, j) and λ_{kjn} for all triplets (k, j, n).

1. Kempter R, Gerstner W, van Hemmen JL (1999) Hebbian learning and spiking neurons. *Phys Rev E* 59:4498–4514.
2. Gerstner W, Kistler WK (2002) *Spiking Neuron Models* (Cambridge Univ Press, Cambridge, UK).
3. Pfister JP, Gerstner W (2006) Triplets of spikes in a model of spike timing-dependent plasticity. *J Neurosci* 26:9673–9682.
4. Brette R (2009) Generation of correlated spike trains. *Neural Comput* 21:188–215.

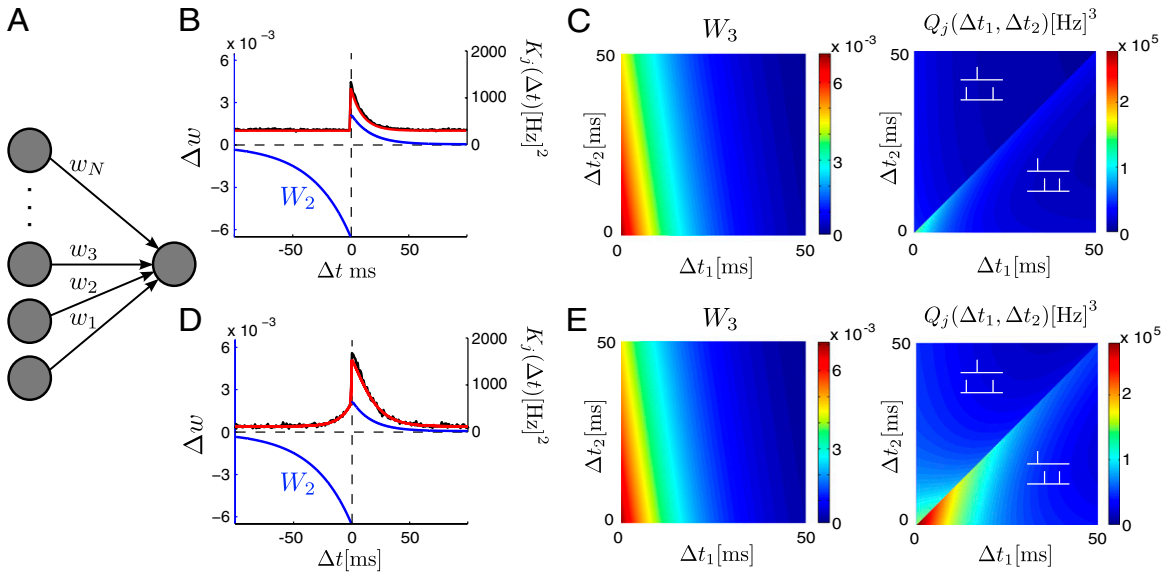

Fig. S1. Weight dynamics depend on pairwise and triplet input correlations. (*A*) The modeling framework consists of a feedforward network of *N* input spiking neurons connected through the weight vector $w = [w_1, \ldots, w_N]^T$ to a single postsynaptic neuron. (*B* and *C*) The weight dynamics in the case of independent Poisson inputs. (*B*) The pairwise contribution to the weight dynamics consists of the integral of the pair-based learning window W_2 (blue line) and the prepost correlation vector K_j (red analytics, black numerics). (*C*) The triplet contribution to the weight dynamics is obtained by multiplying the triplet learning window W_3 (*Left*) with the prepost–post correlation vector Q_j (*Right*). The spike triplets illustrate the particular spike ordering in that region of Q_j. (*D* and *E*) Same as in *B* and *C*, but with exponentially decaying correlated inputs.

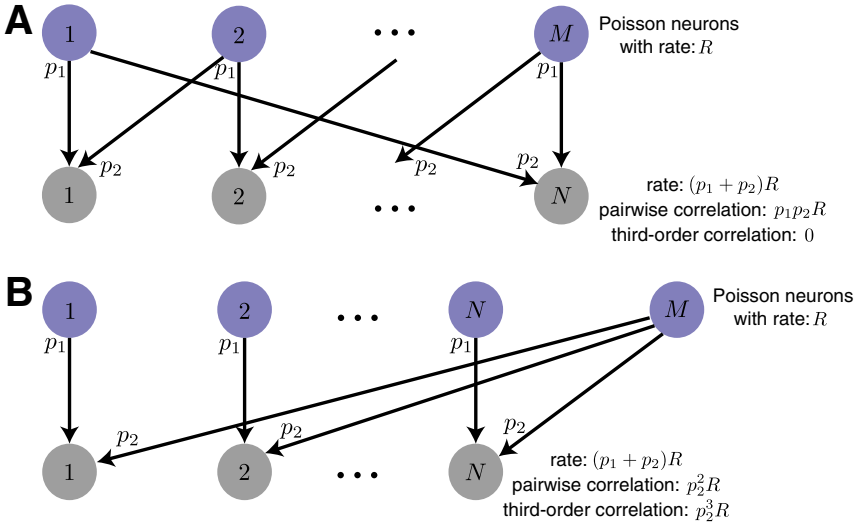

Fig. S2. Generating correlated spike trains. *N* correlated (target) spike trains (gray) were generated by copying spikes from *M* independent Poisson (source) trains (blue) with rates *R*. The coping probability from source train *k* into target train *k* was p_1. (*A*) *N* target spike trains were generated with nonzero pairwise and zero third-order correlations. Correlations arise by copying spikes from a different common source train for each pair of target trains with probability p_2. We show only arrows from the right neighboring source train to each target spike train for clarity. (*B*) *N* target spike trains are generated with nonzero pairwise and third-order correlations. Correlations arise by copying spikes from a single common source train to all target spike trains with probability p_2.

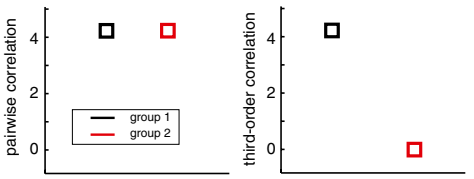

Fig. S3. Correlation strength. The peak correlation strengths (mean for 200 simulation runs) for the two groups of neurons in Fig. 4*C* are shown. (*Left*) Correlation peak for pairwise correlations was very similar for the two groups. Because each group consisted of three inputs, the average of the correlation was computed between any of the three input pairs. (*Right*) Correlation peak for third-order correlations was nonzero for the three inputs in group 1 and zero for the three inputs in group 2.